J. Fluid Mech. (1993), *vol.* 254, *pp.* 649–670
Copyright © 1993 Philips Research

On Marangoni drying: nonlinear kinematic waves in a thin film

By S. B. G. M. O'BRIEN†
Philips Research Laboratories, P.O. Box 80000, 5600 JA Eindhoven, The Netherlands

(Received 24 October 1991 and in revised form 16 March 1993)

In the field of industrial drying, a recent innovation has exploited the occurrence of Marangoni effects in such a way that the resultant free-surface flow enhances the drying process. To this end, alcohol vapour, soluble in water, is introduced above a drying film and as a result of diffusion through the air and water phases a favourable concentration gradient gives rise to the required shear flow. We consider here a simple process driven by this mechanism, and by means of asymptotic simplification and the concepts of singular perturbation theory a leading-order approximation is obtained in which the alcohol concentration in the water is a specified function of space and time. The evolution of the free surface thus reduces to a single nonlinear partial differential equation of a similar form to the Korteweg–de Vries and Burgers equations, higher-derivative terms corresponding to surface tension and gravity effects. Numerical solutions of this equation are obtained and are compared to the application of first order nonlinear kinematic wave theory with corresponding shock solutions.

1. Introduction

If a piece of cotton-wool, saturated with alcohol, is held above the undisturbed surface of a thin film of water, an axisymmetric disturbance occurs in the water in the formation of a ring-shaped wave spreading out from the centre. The observed flow pattern results from the diffusion of alcohol vapour through the air above the film and its subsequent diffusion through the water phase, this giving rise to concentration-dependent surface tension gradients and a corresponding shear-induced flow generally referred to as Marangoni flow. At the Philips Research Laboratories in Eindhoven, these phenomena have recently been exploited for the purpose of speeding up and improving a number of drying processes basically by increasing the maximum speed of dewetting. The term 'Marangoni drying' has been coined for this process, as in Leenaars, Huethorst & Van Oekel (1991), which has the added advantage of being extremely clean: a prerequisite in the microprocessor industry.

If, for definiteness, we consider the case of a silicon wafer being withdrawn from a pool of water (figure 1), then, given good wetting properties (zero contact angle), a thin film of liquid will be entrained on the wafer surface. If, however, the process is carried out in the presence of di-acetone alcohol, the entrained film disappears back into the water and the wafer can be withdrawn almost completely dry. Qualitatively, the mechanism of the drying process arises from the fact that a favourable alcohol concentration gradient is set up near the three-phase line (literally the line at which the three phases – solid, liquid and gas – meet and thus signifying the demarcation line

† Current address: Department of Mathematics, University of Limerick, Ireland.

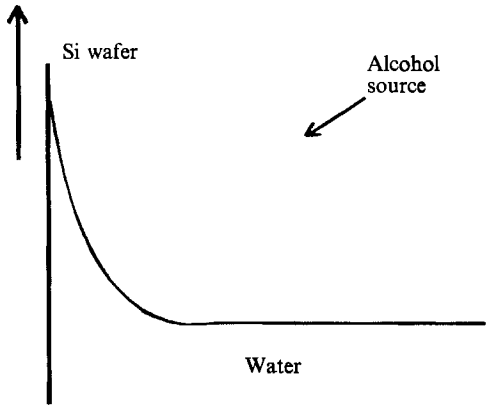

FIGURE 1. Schematic drawing of Marangoni drying process.

between the dry and wet parts of the wafer). A higher concentration generally gives rise to a lower surface tension (see e.g. figure 3 which is a surface tension/concentration curve for *n*-butanol) so the direction of the surface tension gradient and hence the shear stress which is the driving force of the flow is *down* the film. Fluid thus flows back down into the bath and drying is enhanced.

A further application of the same principle can be used during the spin drying of substrates. During spinning, centrifugal forces give rise to an ever-thinning film but removal of the last layer of fluid is traditionally carried out by evaporation. This has the disadvantage that dirt particles originally suspended in the water tend to be left behind on the substrate. If instead alcohol vapour is introduced above the fluid film, it can be observed that the film breaks up into small droplets and rivulets which are more easily spun off the substrate carrying impurities with them. In this case the surface-tension gradients presumably originate as a result of height fluctuations which arise in the film during the spinning. Even if the alcohol flux across the surface is more or less constant, gradients can still arise which ostensibly give rise to instability in the fluid layer: small fluctuations becoming ever larger and eventually developing into droplets.

Marangoni-induced flow has been recognized for some time. The well-known 'kicking' of pendant drops (Haydon 1958) and 'tears of strong wine' effect whereby wine droplets appear mysteriously on the sides of glasses above the liquid surface was first explained by Thomson (1855) though historical credit has gone to Marangoni (1871). This phenomenon bears strong resemblance to the drying problem enunciated above in that the surface-tension gradients are produced by diffusion of solute into (or out of) a solution. In the case of the originally static meniscus in a wine glass, evaporation of alcohol out of the film gives rise to a surface tension gradient in the direction *up* the side of the glass. A thin film thus emerges on the side of the glass above the visible fluid meniscus, giving rise ultimately to the formation of visible droplets which drain back down to the bulk fluid. A further related problem is the drying of paints as considered by Overdiep (1986) who has investigated the problem of whether a paint surface will be conformal to its undersurface or flat irrespective of the form of the latter. He showed that the final film thickness is dependent on a struggle between two factors: the surface tension of the film which favours a flat surface and gradients in the surface tension which tend to result in a conformal coating. One of his results is that the slower a paint film dries out, the flatter the final film, as gradients then become negligible.

Generally speaking, far more attention has been paid to Marangoni instabilities and the interfacial turbulence that results as, for example, in Scriven & Sternling (1960), or to Marangoni flows which arise owing to temperature fluctuations rather than variations in the concentration (Myshkis 1986, chap. 9). A review of the physics involved is given in Levich & Krylov (1969). Pimputkar & Ostrach (1980) consider film flows induced by temperature gradients, but they neglect the smoothing effects of surface tension and, by assuming that gravity smoothing effects are $O(1)$, are restricted to very small curvature situations. In the current paper we are concerned with Marangoni effects which arise due to the presence of a dissolved alcohol and the surface-tension gradients arising from adsorption processes. Adsorption phenomena are not that well understood at present so we use a highly simplified model. In considering a system where the surfactant dissolves fully in the liquid medium, we are in a sense continuing the work of Gaver & Grotberg (1990), Halpern & Grotberg (1992) and Jensen & Grotberg (1992) who restricted attention to liquid surfactants. From a practical point of view, using a vapour allows one to exercise more control over the Marangoni stresses as the distribution of the alcohol can be controlled by introduction of extra alcohol sources (see for example figure 11 of this paper). One thus has better possibilities for controlling the flow. The application described in Leenaars *et al.* (1991) appears to be the first time that Marangoni effects have been exploited to improve a drying process though they have previously been used to enhance mass transfer in two-phase contact units (Patberg *et al.* 1983).

In the course of the paper we demonstrate that Maragoni flow in a thin horizontal film can be reduced to a single nonlinear evolution equation for the free surface which shows some similarity to the Korteweg–de Vries/Burgers equation family in that shock formation is prevented by diffusion and dispersion effects (physically traceable to surface-tension and gravity effects). Benney (1966) showed that flow in a thin film on an inclined plane reduces precisely to the Korteweg–de Vries or Burgers equation in certain limiting cases. In the present paper we show that neglecting the higher-derivative effects gives a reasonable description of the flow even in the case where the insertion of shocks according to kinematic wave theory becomes necessary. In §§2–8 we derive the basic equations describing the flow; §9 is a smoothing layer analysis for those cases where wave steepening occurs; §10 considers some approximate solutions; §11 and, in particular §11.1 describes the numerical solutions of most interest from the fluid mechanics point of view; §11.2 examines numerically the effects of smoothing; and, finally, §12 contains closing remarks.

2. Derivation of equations

We consider first the problem described at the beginning of the paper. We thus have a thin horizontal film of water above which a line source of volatile surfactant is placed (see figure 2). Transport of alcohol through the air is governed by a diffusion equation (convection effects are neglected) while in the water film the flow is driven by the shear stress on the free surface as the alcohol spreads by diffusion and convection. The Stokes equations describe the flow problem; the liquid (water) is assumed incompressible. The relevant equations are

$$\frac{\partial p^*}{\partial x^*} = \mu\left(\frac{\partial^2 u^*}{\partial x^{*2}} + \frac{\partial^2 u^*}{\partial z^{*2}}\right), \tag{1a}$$

$$\frac{\partial p^*}{\partial z^*} = \mu\left(\frac{\partial^2 v^*}{\partial x^{*2}} + \frac{\partial^2 v^*}{\partial z^{*2}}\right) - \rho g, \tag{1b}$$

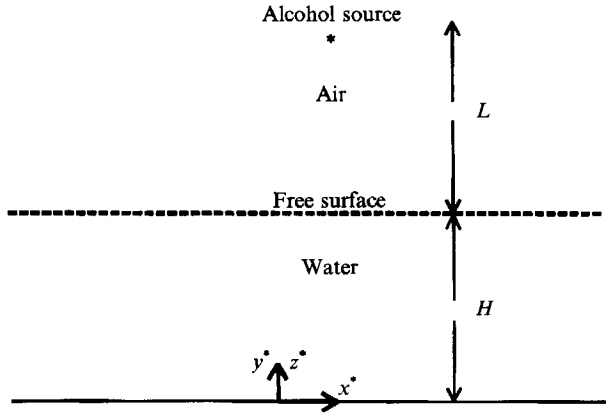

FIGURE 2. Geometry of spreading problem.

where p^* is the pressure, $\boldsymbol{u}^* = (u^*, v^*)$ is fluid velocity in the (x^*, z^*)-directions, μ is the dynamic viscosity (it is assumed that the viscosity of the solution is unaffected by the presence of the alcohol), ρ is the liquid density and g is gravitational acceleration. On the free surface $z^* = h^*(x^*, t^*)$ we have

$$\boldsymbol{t}\cdot(\boldsymbol{\tau}\cdot\boldsymbol{n}) = \frac{\mathrm{d}\gamma^*}{\mathrm{d}C^*}\boldsymbol{t}\cdot\nabla^* C^*, \tag{2}$$

i.e. a concentration-dependent shear stress is exerted on the free surface, $\gamma^* = \gamma^*(C^*)$ being the local surface tension, C^* being the alcohol concentration in the liquid just under the interface in the so-called subsurface; $\boldsymbol{\tau}$ is the stress tensor in the liquid and $\boldsymbol{t}, \boldsymbol{n}$ are local tangential and normal vectors to the free surface. The kinematic condition on $z^* = h^*$ is

$$\frac{\mathrm{D}(z^*-h^*)}{\mathrm{D}t^*} = 0, \quad \text{i.e.} \quad \frac{\partial h^*}{\partial t^*} = v^* - u^*\frac{\partial h^*}{\partial x^*}, \tag{3}$$

while on the substrate noslip yields

$$u^* = 0 \quad \text{on} \quad z^* = 0. \tag{4}$$

The normal stress condition at the free surface, $z^* = h^*(x^*, t^*)$ is

$$\boldsymbol{n}\cdot(\boldsymbol{\tau}\cdot\boldsymbol{n}) = \gamma^*(C^*)\,\Theta^*(x^*, t^*); \quad \Theta^* = h^*_{x^*x^*}/(1+h^{*2}_{x^*})^{\frac{3}{2}}, \tag{5}$$

where Θ^* represents the local curvature of the air/water interface.

For a liquid/gas system containing a third soluble component in equilibrium, there is a discontinuity in the solute concentration across the phase interface. The surface tension of the solution is obtained from the so-called adsorption isotherm and the Gibbs' equation. The solvent molecules migrate towards the interface in order to minimize the free energy: this *adsorption* of molecules at the interface gives rise to a surface concentration that is higher than the bulk concentration and causes a subsequent change in surface tension. If the system is not in equilibrium the situation becomes more complicated as the dynamic surface concentrations cannot generally be obtained from a consideration of the diffusion through the two phases; in addition a time-dependent adsorption model is required. Hansen (1960) assumes that the surface layer is always in equilibrium with the sublayer directly underneath: thus a continual

quasi-equilibrium exists and the rate of adsorption is determined by the diffusion through the bulk phases, no further barriers existing. The equilibrium adsorption isotherms can thus be used. This is the approach used here.

For the alcohol transport in the air, we have

$$D_g\left(\frac{\partial^2 C_g^*}{\partial x^{*2}}+\frac{\partial^2 C_g^*}{\partial y^{*2}}\right)=\frac{\partial C_g^*}{\partial t^*}+\Sigma^*, \tag{6}$$

where C_g^* is alcohol concentration in the air and D_g is the diffusion constant for alcohol vapour in air.

$$\Sigma^*=\lambda\delta(x^*/L,\quad\{y^*-L-H\}/L)\,\delta(t^*/T),$$

where δ is the Dirac distribution, L is distance between the source and the undisturbed liquid free surface (see figure 2), H is initial film thickness, T is a timescale, and λ, a suitable dimensional constant, represents a source term which is elaborated later. In the liquid film the alcohol transport equation is

$$D_l\left(\frac{\partial^2 C^*}{\partial x^{*2}}+\frac{\partial^2 C^*}{\partial y^{*2}}\right)=\frac{\partial C^*}{\partial t^*}+\boldsymbol{u}^*\cdot\nabla C^*, \tag{7}$$

where C^* denotes alcohol concentration in the film, D_l the diffusion constant for alcohol in the liquid and $\boldsymbol{u}^*$ is the velocity vector (u^*, v^*). At the liquid/gas free surface $y^*=h^*(x^*, t^*)$, we have

$$C_g^*=KC^*;\quad D_g\frac{\partial C_g^*}{\partial n}=D_l\frac{\partial C^*}{\partial n}, \tag{8}$$

K representing the partition coefficient at the interface. On the substrate we have a no-flux condition:

$$\frac{\partial C^*}{\partial z^*}=0\quad\text{on}\quad z^*=0. \tag{9}$$

Note that we use a different vertical coordinate (z^*) beneath the liquid surface as the characteristic vertical lengthscale in the water is different than in the gas (denoted y^*). The problem, as it stands, is complicated by the coupling of the flow and alcohol transport problems. We thus first seek simplifications by means of scaling arguments.

3. Scaling of the problem

We non-dimensionalize all variables according to the following scales (starred variables are dimensional):

$$\left.\begin{aligned} x=\frac{x^*}{L},\quad y=\frac{y^*}{L},\quad z=\frac{z^*}{H},\quad h=\frac{h^*}{H},\quad C=\frac{C^*}{C_0},\\ p=\frac{p^*H}{\chi},\quad \chi\Gamma(C)\equiv\chi\left(\gamma(C)-\frac{\gamma_0}{\chi}\right)=-\gamma^*(C^*),\\ u=\frac{u^*\mu L}{H\chi},\quad v=\frac{v^*\mu L^2}{\chi H^2},\quad t=\frac{\chi H t^*}{\mu L^2}. \end{aligned}\right\} \tag{10}$$

The lengthscale L is a characteristic scale imposed by the alcohol source and is taken to be the distance between source and film, H is the initial film thickness, C_0 is a characteristic concentration obtained from a surface-tension curve as in figure 3, γ_0 is

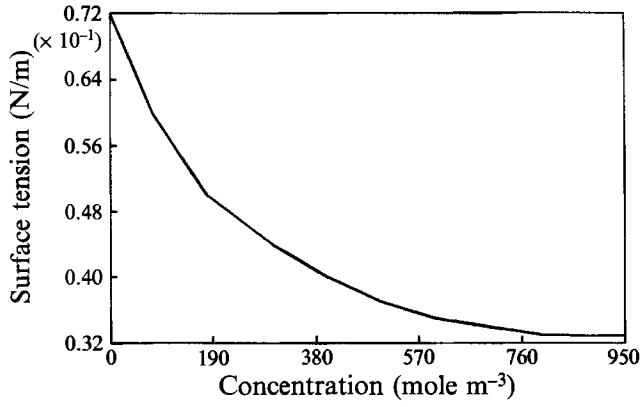

FIGURE 3. Surface tension/concentration curve for *n*-butanol.

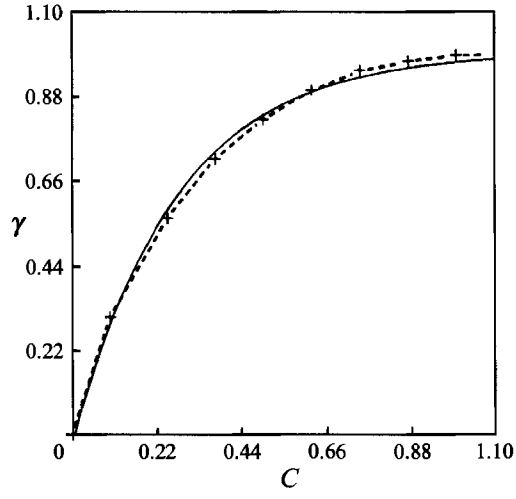

FIGURE 4. Dimensionless surface tension/concentration curve for *n*-butanol: --+--, experimental; ——, curve fit.

the surface tension of pure water, χ is the so-called spreading pressure defined by $\chi = \gamma_0 - \gamma_s$ where γ_s is the minimum surface tension (i.e. the surface tension of pure surfactant) apparent in figure 3.

As the quantities in figure 3 are dimensional, some care must be taken in transforming to dimensionless quantities. For example the relationship between γ^* and C^* might be written $\gamma^* = f(C^*)$ but this relationship is only correct for one set of units. By non-dimensionalizing γ^* and C^* we obtain a relationship such as $\gamma = g(C)$ which is correct in our chosen set of units, i.e. the reference scales for C^* and γ^*. In the course of the analysis, it is necessary to have expressions for $\gamma(C)$ and its derivatives with respect to C, i.e. γ_c, γ_{cc}, etc. If we take the non-dimensional form of figure 3, we obtain a curve as shown in figure 4, noting that there is a change in the sign of the slope due to the particular scaling chosen ($\gamma^*(C^*)$ and $\gamma(C)$ have opposite signs in (10)). Applying an exponential least-squares curve fit to this data gives the result $\gamma(C) = 1 - 1.02\exp(-3.6C)$ for *n*-butanol. The curve fit is also shown in figure 4. In view of this it is not unreasonable to represent a universal alcohol by the curve $\gamma(C) = 1 - \exp(-SC)$, where S is varied to represent different alcohols. For example, ethanol (respectively *n*-

hexanol) shows a less (more) extreme surface-tension curve than *n*-butanol and this will be reflected in a smaller (larger) value of S. The surface-tension variation for ethanol is thus considerably smaller and it gives rise to significantly smaller disturbances.

The scale for the pressure is obtained by comparison of the two leading-order terms in (1*a*) and it is noteworthy that this scale varies inversely with the film thickness. Physically this means that the pressure developed in a thin film by the Marangoni stresses is much larger than, say, the hydrostatic pressure. This is the reason why the process works so well: the driving forces are relatively large. The scale for the velocity is obtained by an estimate of the velocity on the free surface in (1) without surface tension ($\mathrm{d}p/\mathrm{d}x = 0$, i.e. Couette flow) when the shear stress is maximal, and the timescale follows directly from this. An alternative diffusion timescale would be L^2/D_g but this turns out to be numerically of the same order as the chosen scale. Note that for water $\mu = 10^{-3}\ \mathrm{kg\,m^{-1}\,s^{-1}}$, $\chi \approx 4\times 10^{-2}\ \mathrm{Nm^{-1}}$, while $D_g \approx 10^{-5}\ \mathrm{m^2\,s^{-1}}$ and H is generally not smaller than 1 μm. At this point, for reference, we also include typical values for the other parameters in the problem: C_0 from figure 3 is about 900 mole $\mathrm{m^{-3}}$ while γ_0 for water is about $7.26\times 10^{-2}\ \mathrm{Nm^{-1}}$, $D_l \approx 10^{-9}\ \mathrm{m^2\,s^{-1}}$, $L \geqslant 10^{-3}$ m. This latter lengthscale represents distance from the source to the free surface (see figure 2).

Equations (1)–(9) in scaled form become

$$\frac{\partial p}{\partial x} = \epsilon^2\frac{\partial^2 u}{\partial x^2}+\frac{\partial^2 u}{\partial z^2}, \tag{11a}$$

$$\frac{\partial p}{\partial z} = \epsilon^4\frac{\partial^2 v}{\partial x^2}+\epsilon^2\frac{\partial^2 v}{\partial z^2}-\epsilon^2 B, \tag{11b}$$

with boundary conditions

$$\frac{\partial u}{\partial z} = -\gamma_x + O(\epsilon^2) \quad \text{on} \quad z = h(x,t) \tag{12}$$

$$u = 0 \quad \text{on} \quad z = 0, \tag{13}$$

where in (12), it is understood that $\gamma_x = \gamma_c C_x$;

$$p = \epsilon^2 \Gamma h_{xx} \quad \text{on} \quad z = h(x,t) \tag{14}$$

with Γ as defined in (10), i.e. $\Gamma(C) = \gamma(C) - \gamma_0/\chi$;

$$\left(\frac{\partial^2 C_g}{\partial x^2}+\frac{\partial^2 C_g}{\partial y^2}\right) = P_1\frac{\partial C_g}{\partial t}+\Sigma, \tag{15}$$

$$\epsilon^2\frac{\partial^2 C}{\partial x^2}+\frac{\partial^2 C}{\partial z^2} = \epsilon^2 P_2\left(\frac{\partial C}{\partial t}+u\frac{\partial C}{\partial x}+v\frac{\partial C}{\partial z}\right), \tag{16}$$

with boundary conditions

$$C_g = C; \quad \epsilon DK\frac{\partial C_g}{\partial y} = \frac{\partial C}{\partial z} \quad \text{on} \quad z = h(x,t), \quad y = \epsilon h(x,t), \tag{17}$$

$$\frac{\partial C}{\partial z} = 0; \quad y = \infty, \quad C_g = 0 \quad \text{on} \quad z = 0, \tag{18}$$

$$\frac{\partial h}{\partial t} = v - u\frac{\partial h}{\partial x}. \tag{19}$$

In (16) and (17), C has been rescaled such that $KC \to C$ where K is assumed $O(1)$. The case where $K \gg 1$ would be essentially the same while $K \ll 1$ would require a slightly

different treatment. In addition $\epsilon = H/L$, $B = \rho g L^2/\chi$ is a Bond number indicating the relative importance of gravity and surface tension, $D = D_g/D_l$, and $P_1 = \chi H/D_g\mu$, $P_2 = \chi H/D_l\mu$, the last two parameters being Péclet numbers though P_1 compares properties in two different phases. P_2 is a measure of the relative importance of convection and diffusion in the liquid.

4. Limiting cases

There are a number of simplifications which we can make to (11)–(19) by considering limiting processes. Letting $P_1 \to 0$ or ∞ in (15) yields a quasi-static or time-independent C_g respectively. More interestingly, letting $\epsilon^2 P_2 \to 0$ in (16) yields a situation where convection effects in the film are dominated by diffusion and the alcohol transport problem in the film is considerably simplified. The case where $\epsilon^2 P_2 \to \infty$ with ϵ^2 held fixed yields a first-order partial differential equation for the alcohol concentration. Simplification of (17) should be approached with care because if, for example, we consider $\epsilon D \to 0$ or ∞ then such cases can physically correspond to either liquid or solid being a perfect 'conductor'. Using the parameter values of §3 as a rough guide suggests that a relevant limiting situation for the problem at hand is given by $\epsilon \to 0$, $\epsilon^2 P_2 \to 0$; $\epsilon D = O(1)$; $\epsilon^2 B \to 0$. The rest of the paper considers this situation, and slight variations on it, in some detail so if the parameters in a particular instance numerically satisfy the conditions of the previous sentence, the analysis which follows is expected to be valid.

5. The leading-order flow problem

We now proceed to simplify the flow equations (11)–(14) by exploiting the smallness of the aspect ratio ϵ so developing a lubrication approximation for the flow. At this point we stress that the intention of the analysis that follows is to obtain a leading-order approximation to the problem stated in §4 with an error $o(1)$. As will also become clear, this straightforward perturbation represents a singular limit in that certain terms which formally appear to be $o(1)$ change order and must be included in the $O(1)$ analysis.

We now seek solutions to (11*a*, *b*) in the form

$$u = u_0 + \epsilon^2 u_1; \quad v = v_0 + \epsilon^2 v_1; \quad p = p_0 + \epsilon^2 p_1. \tag{20}$$

To zero order we easily obtain

$$u_0 = -\gamma_x z; \quad v_0 = \tfrac{1}{2}\gamma_{xx} z^2; \quad p_0 = 0, \tag{21a–c}$$

while to first order we get

$$u_1 = \Gamma h_{xxx}(\tfrac{1}{2}z^2 - hz) + B h_x(\tfrac{1}{2}z^2 - hz) + O(N), \tag{22a}$$

$$v_1 = \Gamma h_{xxxx}(\tfrac{1}{3}z^3) + \tfrac{1}{2}\Gamma h_{xxx} h_x z^2 - B h_{xx}(\tfrac{1}{6}z^3 - \tfrac{1}{2}hz^2) + \tfrac{1}{2}B h_x^2 z^2 + O(N), \tag{22b}$$

$$p_1 = \Gamma h_{xx} + B(h - z) + O(N), \tag{22c}$$

where the notation $O(N)$ is used to indicate terms making contributions which are always strictly $o(1)$ and thus remain negligible even in the smoothing layer. It is important to note that in deriving (22), we have used the fact that γ, γ_x, γ_{xx} etc. all remain $O(1)$ which may be verified by examining (28) bearing in mind that $C(x, t)$ is correct to $O(\epsilon)$. We also comment that the correctness of (22) only becomes completely obvious after the smoothing-layer analysis of §9 has been carried out.

To verify that the basic idea is correct, most of the numerical solutions of §11.2.2 were also carried out while including some of the $O(N)$ terms of (22). The results were

indistinguishable from those obtained neglecting all $O(N)$ terms. In (22), terms containing the factor B give rise to gravity smoothing, while $O(\epsilon^2)$ terms containing higher derivatives of h will cause similar surface-tension effects. The $O(B)$ terms can only play a role at leading order if B is large enough, as discussed in §9.

6. Asymptotic simplification of the diffusion problem

The simplified version of (16) is now just

$$\partial^2 C/\partial z^2 = O(\epsilon^2, \epsilon^2 P_2) \tag{23}$$

and this in conjunction with the boundary condition (18) yields

$$\partial C/\partial z = O(\epsilon^2, \epsilon^2 P_2) \tag{24}$$

throughout the liquid film. The film is thus thin enough that diffusion in the vertical direction occurs so quickly that the concentration gradient in this direction is always negligible. Boundary conditions (17) now become

$$C_g = C, \quad \partial C_g/\partial y = o(1) \tag{25a, b}$$

on the free surface $z = h(x, t)$, $y = \epsilon h(x, t)$. In §4 we suggested that $\epsilon D = O(1)$ would be an appropriate limiting value, in which case the error in (25*b*) would be $O(\epsilon^2)$. For the leading-order approximation which we seek, this correction is academic. From (24) and (25*a*), the alcohol concentration in the liquid is just

$$C(x, t) = C_g(x, \epsilon h, t) + O(\epsilon^2, \epsilon^2 P_2) \quad \text{or} \quad C(x, t) = C_g(x, 0, t) + O(\epsilon) \tag{26}$$

using a Taylor series expansion. This greatly simplifies the problem as it means that the film is thin enough for the no-penetration condition pertaining to the alcohol at the substrate to be 'moved' to the free liquid surface. We thus reduce to a search for a solution of (11)–(14) with C and C_g known everywhere in space and for all time. Owing to this uncoupling, the evolution of the free surface reduces to a single partial differential equation (of fourth order).

Note further that the results of this section would also be valid for the limiting situation $\epsilon D \gg 1$, $\epsilon^2 P_2 = O(1)$, which might occur if D_l was an order of magnitude smaller ($= 10^{-10}\,\mathrm{m^2\,s^{-1}}$). The point is that even though the $O(\epsilon^2 P_2)$ terms of (16) complicate the alcohol transport problem in the liquid layer, only the concentration of alcohol in the interface is required to determine the Marangoni forces. For large ϵD, (17) indicates that from the point of view of the air, $\partial C_g/\partial y \ll 1$ at the free surface regardless of what happens in the water and so the diffusion problem in the air still reduces to that described above.

7. Evolution of the free surface

The time-dependent evolution of the free-surface profile is given by (19), (21) and (22) and may be written as

$$h_t = \tfrac{1}{2}\gamma_{xx} h^2 + \gamma_x h h_x + \epsilon^2 B(\tfrac{1}{3} h_{xx} h^3 + h^2 h_x^2) + \epsilon^2 \Gamma(\tfrac{1}{3} h_{xxxx} h^3 + h_{xxx} h^2 h_x). \tag{27}$$

Of course (27), an evolution equation for h, looks rather unappealing being highly nonlinear and having rather complicated coefficients. Further progress can only be made by numerical means. Equation (27) can be regarded as a sort of generalized Korteweg–de Vries/Burgers equation though it also contains some fourth-derivative diffusive terms. If we initially ignore the terms of $O(\epsilon^2, \epsilon^2 B)$ we have the sort of equation

that occurs in the study of nonlinear kinematic waves (Whitham 1974) which is physically what we might expect. We expect to get a wave moving in both directions away from the z-axis. The alcohol concentration in the film has a maximum at $x = 0$ and decreases monotonically as $|x|$ increases. Figure 3 shows that a high alcohol concentration in the water yields a relatively lower surface tension so the surface tension increases with increasing $|x|$. Flow occurs in the direction of increasing surface tension so a twin wave can be expected to move out away from the z-axis. To verify that this is indeed the effect of the first-order terms, we will derive some approximate solutions in §10, before proceeding to full numerical solutions in §11.

We can get some insight into the formation of shocks occurring in the reduced form of (27) by considering the theoretical limiting case of large P_1. In this case, the timescale of the film response is much shorter than the diffusion timescale in the gas. Thus, on the timescale of the flow in the film, changes in surface tension are slow so γ, γ_x, γ_{xx} are approximately time-independent. Using the transformation

$$\eta = |\gamma_x|^{\frac{1}{3}} h; \quad \mathrm{d}x/\mathrm{d}\xi = |\gamma_x|^{\frac{1}{3}},$$

(27) with $\epsilon^2 B = \epsilon = 0$ becomes

$$\eta_t + \eta\eta_\xi = 0$$

with initial condition $\eta(\xi, t = 0) = |\gamma_x|^{\frac{1}{3}}|_{x \to \xi}$. This represents a nonlinear wave moving with wave speed η and whether it breaks or not depends entirely on the initial data and in particular whether $\eta_\xi(\xi, 0)$ changes sign at any point. But $\eta_\xi(\xi, 0) = -\frac{1}{2}\gamma_{xx} = -\frac{1}{2}(\gamma_x)_x$ so if $-\gamma_x$ has a turning point (maximum) in $0 < x < \infty$ for all times $0 < t < \infty$ (as is the case for example in the special solutions examined in the next section) then shocks will always form (and breaking first occurs when $2/(\gamma_{xx})$ has its smallest positive value as in Whitham 1974). The physical relevance of $-\gamma_x$ having a maximum is that the velocity to leading order on the free surface is proportional to $-\gamma_x$ (see (21 a)), and if this velocity is decreasing at any point for increasing x, liquid from behind tends to catch up and shocks form. This is further discussed in §10. Note finally that (27) is correct for all surfactant distributions: we now consider the case of a single line source.

8. Solution for the case of a line source of surfactant

We now specialize the problem of surfactant diffusion through the air to that represented schematically in figure 2 where a line source of surfactant has been placed at (0, 1), obtaining the following approximate solution:

$$C_g(x, y, t) = \frac{A}{t}\left[\exp\left\{\frac{-(x^2 + [y-1]^2)\,P_1}{4t}\right\} + \exp\left\{\frac{-(x^2 + [y+1]^2)\,P_1}{4t}\right\}\right]. \tag{28}$$

In the liquid film the concentration is independent of the vertical coordinate as evidenced by (24), and from (26) we get

$$C(x, t) = \frac{2A}{t}\exp\left\{\frac{-(x^2+1)\,P_1}{4t}\right\} + O(\epsilon), \tag{29}$$

where A is a dimensionless constant representing the strength of the source. If the total amount of alcohol deposited in the air phase at $t^* = 0$ is M^* moles, then we define $M = M^*/(L^2 C_0)$ and A is related to M by

$$M = \int_0^\infty \int_{-\infty}^\infty C_g(x, y, t)\,\mathrm{d}x\,\mathrm{d}y = \frac{4\pi A}{P_1}. \tag{30}$$

In the remainder of the paper the influence of the alcohol source represented in this section will be considered in some detail.

9. Smoothing-layer equations

As already pointed out in §5, the asymptotic simplifications of this paper are based on the presumption of smoothing-layer behaviour in regions where the free-surface slope becomes large. The numerical solutions of §11 show that the first-order terms of (27) develop shocks. These can be smoothed out by the higher-derivative terms. For such terms formally to have any influence on (27), we require a rescaling of x. A suitable smoothing-layer coordinate is given by

$$x - x_s(t) = \delta\xi, \tag{31}$$

as suggested by Kevorkian & Cole (1981). We thus transform coordinates from (x, t) to (ξ, t) according to the following rules:

$$\frac{\partial}{\partial t} = -\frac{1}{\delta}\dot{x}_s(t)\frac{\partial}{\partial \xi} + \frac{\partial}{\partial t}; \quad \frac{\partial}{\partial x} = \frac{1}{\delta}\frac{\partial}{\partial \xi}, \tag{32}$$

where the dot signifies differentiation with respect to t. In the smoothing-layer region, the x-coordinate is stretched as in (31) and an inner equation and solution obtained. The inner and outer solutions (obtained from (27) without higher derivatives) can then be matched numerically as in Moriarty, Schwartz & Tuck (1991). As numerical solutions of the full equation (27) are not difficult to find, we only attempt to write down the smoothing-layer equations. In doing so, we will be able to provide justification for the assumptions of §5.

We consider first the richest possible smoothing-layer structure where gravity and surface tension provide equal smoothing effects. We have already commented in §5 that (29) and (31) can be used to show that $\gamma_x (= \gamma_c C_x)$, γ_{xx} and higher derivatives are $O(1)$ in the smoothing layer. This is very significant because it means that only derivatives of h can give rise to 'scaled up' terms in this layer. This is also the origin of the $O(N)$ terms of §5: in order to identify terms of relevance in the smoothing layer, it is only necessary to examine derivatives of h. This is also physically justified: derivatives of γ produce the Marangoni driving force for the flow; this would not be expected to dramatically increase where the wave steepens. Using (32) and (27) we thus arrive at

$$h_t - \frac{1}{\delta}\dot{x}_s(t)\,h_\xi = \tfrac{1}{2}\gamma_{xx}h^2 + \frac{1}{\delta}\gamma_x hh_\xi + \frac{\epsilon^2 B}{\delta^2}(\tfrac{1}{3}h_{\xi\xi}h^3 + h_\xi^2 h^2) + \frac{\epsilon^2}{\delta^4}\Gamma(\tfrac{1}{3}h_{\xi\xi\xi\xi}h^3 + h^2 h_\xi h_{\xi\xi\xi}). \tag{33}$$

In this situation, a dominant balance with gravity and surface-tension forces of the same order arises when

$$B = O(\epsilon^{-\frac{4}{3}}); \quad \delta = \epsilon^{\frac{2}{3}}, \tag{34}$$

and the smoothing-layer equation is given by

$$-\dot{x}_s(t)\,h_\xi = \gamma_x hh_\xi + \tfrac{1}{3}h_{\xi\xi}h^3 + h^2h_\xi^2 + \Gamma(\tfrac{1}{3}h_{\xi\xi\xi\xi}h^3 + h^2h_\xi h_{\xi\xi\xi}). \tag{35}$$

Derivatives of γ have been written in terms of x to emphasize that γ does not change order in the smoothing layer.

Proceeding to the case where smoothing is caused predominantly by surface tension, we take $B = O(1)$ or $B \ll 1$ and a dominant balance is obtained when

$$\delta = \epsilon^{\frac{2}{5}}, \tag{36}$$

the relevant smoothing-layer equation being

$$-\dot{x}_s(t)\,h_\xi = \gamma_x hh_\xi + \Gamma(\tfrac{1}{3}h_{\xi\xi\xi\xi}h^3 + h^2h_\xi h_{\xi\xi\xi}). \tag{37}$$

Note that the numerical solutions appropriate to this case (figure 14) suggest that smoothing effects are not just restricted to a thin layer. However, we would still expect the highest-derivative terms to be the most relevant. In the case where smoothing is only caused by gravity effects, we take $\epsilon \to 0$, $\epsilon^2 B$ finite. The required smoothing-layer scaling occurs when

$$\delta = \epsilon^2 B, \tag{38}$$

giving rise to the following smoothing-layer equation:

$$-\dot{x}_s(t)\, h_\xi = \gamma_x h h_\xi + \tfrac{1}{3} h_{\xi\xi} h^3 + h^2 h_\xi^2. \tag{39}$$

10. Small-slope approximations

We consider three situations which are all quite similar in their requirement of small wave slope. With this in mind, we neglect the higher-derivative terms and consider just the $O(1)$ terms of (27) which we write as

$$h_t = \tfrac{1}{2}\gamma_{xx} h^2 + \gamma_x h h_x + O(\epsilon^2, \epsilon^2 B). \tag{40}$$

For small concentrations we write

$$C(x,t) = 0 + \beta C_1(x,t); \quad h(x,t) = h(x,0) + \beta h_1(x,t), \tag{41}$$

where β is some small number. By small we mean that in figure 4, where $\gamma = \gamma(C)$, if the concentration varies from its original value $C = 0$ by an amount of $O(\beta)$, then the $\gamma(C)/C$ curve can be linearized about the zero value $\gamma_0 = \gamma(C = 0)$. In this range we thus have $\gamma = SC$; $\gamma_c = S$; $\gamma_{cc} = 0$, where S is the initial slope of the surface-tension curve. Note that the sign of γ_c is different from that of $\gamma_{c^*}^*$ due to the choice of scales (10). If the undisturbed film is given by $h(x,0) = 1$, then we obtain the following equation for h_1:

$$h_1 = \tfrac{1}{2} S \int_0^t \frac{\partial^2 C_1}{\partial x^2}\, \mathrm{d}t, \tag{42}$$

where $\partial^2 C/\partial x^2$ is obtained from (29) with $A = \beta$. We thus obtain the result

$$h_1 = \frac{P_1 S}{2\alpha} \exp\left\{-\frac{\alpha}{t}\right\}\left[\frac{P_1 x^2}{2\alpha}\left(\frac{\alpha}{t} + 1\right) - 1\right], \tag{43}$$

with $\alpha = \frac{1}{4}(x^2 + 1) P_1$, This solution is generated exclusively by the first term on the right-hand side of (40).

We can obtain a similar asymptotic result, useful for checking numerical results, by examining the small-time behaviour of (40). For small times we expect small deviations in the film shape from its undisturbed profile. We scale as follows:

$$t = \beta T; \quad h = 1 + H, \tag{44}$$

where β is an arbitrary small parameter. The scale of the perturbation $H(x,t)$ in the film is as yet unknown but will certainly be $o(1)$. Equation (40) now becomes

$$\frac{1}{\beta}\frac{\partial H}{\partial T} = \frac{S}{2}\left[\frac{P_1^2 x^2}{4\beta^2 T^2} - \frac{P_1}{2\beta T}\right]\frac{2A}{\beta T} \exp\left[\frac{-(x^2+1) P_1}{4\beta T}\right] + \text{higher-order terms} \tag{45}$$

yielding the solution

$$H(\beta T, x) = \frac{P_1 A S}{2\alpha} \exp\left[\frac{-\alpha}{\beta T}\right]\left(\frac{P_1 x^2}{2\alpha}\left[\frac{\alpha}{\beta T} + 1\right] - 1\right), \tag{46}$$

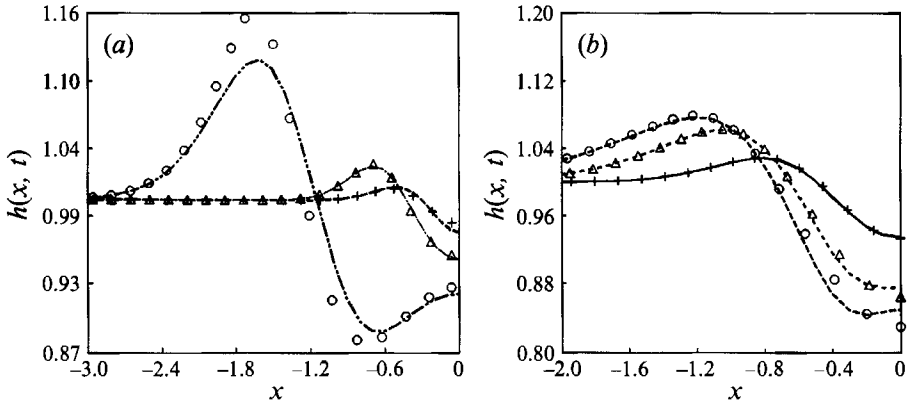

FIGURE 5. (*a*) Comparison of perturbation and numerical solutions. $A = 1$, $P_1 = 1$, $S = 2$. Numerical: +, $t = 0.05$; △, $t = 0.07$; ○, $t = 0.3$. Equation (46): ---, $t = 0.05$; Equation (47): —·—, $t = 0.07$; —··—, $t = 0.3$. (*b*) Comparison of small-S perturbation and numerical solutions. $A = 1$, $P_1 = 4$, $S = 0.2$. Numerical: +, $t = 0.6$; △, $t = 1.2$; ○, $t = 1.8$. Equations (50)–(53): ——, $t = 0.6$; ---, $t = 1.2$; ———, $t = 1.8$.

where $\alpha = \alpha(x)$ is as defined above. This is very similar to (43): the disturbance in this instance being exponentially small in β. Checking back to (45) it is easily verified, *a posteriori*, that the neglected terms are indeed negligible. Some results are plotted in figure 5(*a*) comparing (46) with numerical solutions (obtained by solving the complete version of (27)).

It is useful at this point to derive some results for the alcohol concentration in the film. The maximum value of the concentration occurs when $\partial C/\partial x = 0$ and $\partial C/\partial t = 0$. From (29) it is easy to show that this occurs when $x = 0$ (which is intuitively obvious) and $t = \frac{1}{4}P_1$. The maximum value is given by $8A\exp(-1)/P_1$. When $A = 1$, $P_1 = 1$, $C_{max} = 2.943$, while for $A = 1$, $P_1 = 4$, $C_{max} = 0.736$. For the first of these situations this indicates that at the very least we require $\beta T \ll 0.25$ in order for (46) to be valid, i.e. in order that $C(x, t) = o(1)$. In fact, figure 5 shows that the perturbation solution (46) is good for $\beta T = 0.05$. However, it turns out that it deviates considerably for $\beta T = 0.07$. In particular, the error in the solution at the lowest point of the film is a considerable overestimate. This can easily be understood by consideration of figure 4. The driving force of the flow is determined by the gradient of the surface tension; this is largest for small concentrations but for high enough concentrations becomes small. As the perturbation solution uses the initial slope as a first estimate it clearly will overestimate the flow for larger concentrations. We can improve the small-time estimate by using the full form of the surface-tension curve in the form: $\gamma(C) = 1-\exp(-SC)$ as already discussed. In this instance we obtain the following equation for $H(x, t)$:

$$\frac{\partial H}{\partial t} = \tfrac{1}{2}\exp[-SC(x,t)]\left\{S\frac{\partial^2 C}{\partial x^2} - S^2\left(\frac{\partial C}{\partial x}\right)^2\right\}. \tag{47}$$

This equation can be solved by numerical quadrature and the improved estimate at $t = 0.07$ as shown in figure 5(*a*) is indistinguishable from the numerical solution. In fact (47) gives reasonable results even up to $t = 0.3$ as also shown in figure 5(*a*). The underestimate of the wave height arises because the wave slope is large at this point.

For very long times it is clear that (40) reduces to $\partial h/\partial t = 0$ as all concentration gradients disappear. The film is then frozen in its final position. In reality this does not

happen: a disturbed film as in figure 5(*a*) falls back in on itself if there is no longer any driving force. The terms that cause this – the $O(\epsilon^2 B)$ terms which represent the flattening effects of gravity and the $O(\epsilon^2)$ effects representing the smoothing effects of surface tension in (27) – can then no longer be neglected. For the range of values under consideration here, this recovery occurs on a rather longer timescale (see §11.2) than the Marangoni flow, i.e. the recovery takes place very slowly.

We can also derive asymptotic results by considering the situation where $S \ll 1$. This physically corresponds to a weakly surface-active alcohol. In this instance we simplify the expressions for the surface tension/concentration curve and its derivatives, obtaining

$$\gamma(C) \approx sC - \tfrac{1}{2}s^2C^2; \quad \gamma_c(C) \approx s - s^2C; \quad \gamma_{cc}(C) \approx -s^2, \tag{48}$$

writing $s(\ll 1)$ for S. If we now seek solutions of the form

$$h(x,t) = h_0 + sh_1 + s^2h_2 \tag{49}$$

we obtain the following equations from (27):

$$\frac{\partial h_0}{\partial t} = 0; \quad \frac{\partial h_1}{\partial t} = \frac{1}{2}\frac{\partial^2 C}{\partial x^2}; \tag{50a, b}$$

$$\frac{\partial h_2}{\partial t} = -\frac{1}{2}\left(\frac{\partial C}{\partial x}\right)^2 + \frac{\partial C}{\partial x}\frac{\partial h_1}{\partial x} + \frac{\partial^2 C}{\partial x^2}(h_1 - \tfrac{1}{2}C), \tag{51}$$

with initial conditions

$$h_0(x,0) = 1; \quad h_1(x,0) = 0; \quad h_2(x,0) = 0. \tag{52}$$

Equation (50) can be solved in closed form and this yields

$$h_0 = 1; \quad h_1 = \frac{1}{2}\frac{P_1 A}{\alpha}\exp\left(-\frac{\alpha}{t}\right)\left(\frac{P_1 x^2}{2\alpha}\left\{\frac{\alpha}{t}+1\right\} - 1\right), \tag{53a, b}$$

where (53*b*) is essentially the same as (46). Equation (51) is solved by numerical quadrature as C and its derivatives are known functions. In figure 5(*b*) we compare the results of this perturbation analysis with numerical solutions. The results are seen to be very good for all times. Referring back to (48), which exploits the smallness of s, we note that in fact it is sC that must be numerically small. It is thus necessary to check that $sC_{max} = s8A\exp(-1)/P_1$ is small. For this reason, the case where $P_1 = 1$ requires smaller values of s to obtain the same accuracy as when $P_1 = 4$.

It is instructive to consider (40) for the case of small $S(= s)$ by the method of characteristics. The following equations are obtained:

$$\frac{\mathrm{d}x}{\mathrm{d}t} = -h(s - s^2C)\frac{\partial C}{\partial x}, \tag{54}$$

$$\frac{\mathrm{d}h}{\mathrm{d}t} = \tfrac{1}{2}h^2(-s^2 + s^3C)\left(\frac{\partial C}{\partial x}\right)^2 + \tfrac{1}{2}h^2(s - s^2C)\frac{\partial^2 C}{\partial x^2}. \tag{55}$$

If we seek solutions $x = x_0 + sx_1$; $h = h_0 + sh_1$, to lowest order the characteristic equation (54) reduces to $\mathrm{d}x_0/\mathrm{d}t = 0$, which indicates that the characteristic curves are non-intersecting straight lines in the limit $s \to 0$. Thus the asymptotic solution can never represent a breaking wave: the characteristics never intersect. This can also be inferred from (50) and (51) due to the absence of nonlinear terms in h.

11. Numerical solutions

We proceed now to examine the behaviour of the full evolution equation (27). In doing this we treat (27) as a model equation and examine its behaviour for different values of $\epsilon^2 B$ and ϵ without being too fussy as to whether these values arise in practice or not. In practice, $\epsilon^2 B$ can be as small as 10^{-5} in some instances but we only try to demonstrate the effects of the different terms and the trends resulting from varying the different parameters.

As noted in §6, the driving force of (27) is given by the first-order terms as evinced by (40). This is a first-order nonlinear partial differential equation. A suitable initial condition is given by

$$h(x,0) = 1; \quad C(x,0) = 0; \tag{56}$$

though the condition for the concentration is implicitly contained in (29). Numerically we deal with this condition by allowing the diffusion process to develop for some small time (e.g. $t = 10^{-6}$), before flow occurs. The first-order terms of (27) can develop shocks, which physically corresponds to a steepening of the liquid free surface until a jump discontinuity is formed. The techniques for describing such a situation are well-known (Whitham 1974). Physically, the occurrence of such shocks indicates a breakdown of the mathematical model. Thus (27) describes the initial development of the wave front, but only remains valid for all time if the wave does not become too steep. We distinguish between three different cases:

case (i) no smoothing;

case (ii) gravity smoothing via $O(\epsilon^2 B)$ terms;

case (iii) gravity and surface-tension smoothing via $O(\epsilon^2 B)$ and $O(\epsilon^2)$ terms.

11.1. *Case (i): Marangoni flow, no smoothing*

In this case $\epsilon^2 B = 0$, $\epsilon = 0$. The problem can be treated numerically by applying the method of characteristics. Equation (27) is hyperbolic and reduces to the following system of coupled ordinary differential equations:

$$\mathrm{d}x/\mathrm{d}t = -h\gamma_c C_x, \tag{57}$$

$$\mathrm{d}h/\mathrm{d}t = \tfrac{1}{2}h^2(\gamma_{cc} C_x^2 + \gamma_c C_{xx}). \tag{58}$$

The first of these defines the characteristic curves where $C(x,t)$ and its derivatives are defined by (29). The corresponding initial conditions are:

$$x(0) = \xi; \quad h(0) = 1, \tag{59}$$

where ξ runs from $-\infty$ to $+\infty$. In practice we choose $\xi \in [-10, 10]$ and (57) and (58) are solved numerically at a number of points in this interval.

A typical set of results is shown in figure 6. In general we distinguish between two generic cases: no-breaking and breaking, the latter possibility having already been briefly discussed in §7. Figure 6 indicates that the film height does not attain its minimum at the axis of symmetry ($x = 0$). The film does exhibit some thinning at this point but the minimum is obtained at about $x = -1.6$ and this minimum moves outwards with the wave. The alcohol concentration is somewhat higher at $x = 0$ than $x = -1.6$ and referring to figure 4, we can expect larger gradients in the surface tension (and hence a larger driving force and thinner film) at $x = -1.6$. Referring to the small-time solutions of figure 5(*a*), we see that here the low point of the free surface *does* initially occur at $x = 0$ because for small times the γ/C curve is essentially a straight line so that higher concentrations give rise to a higher driving force. Note that, in the case of figure 6, the wave does not break if we carry on the integration further in time

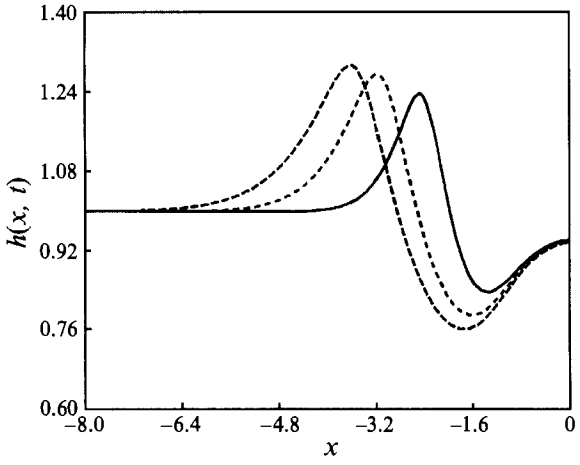

FIGURE 6. Case (i) no breaking, $A = 1$, $P_1 = 1$, $S = 4$. ——, $t = 0.6$; – – –, $t = 1.2$; ———, $t = 1.8$.

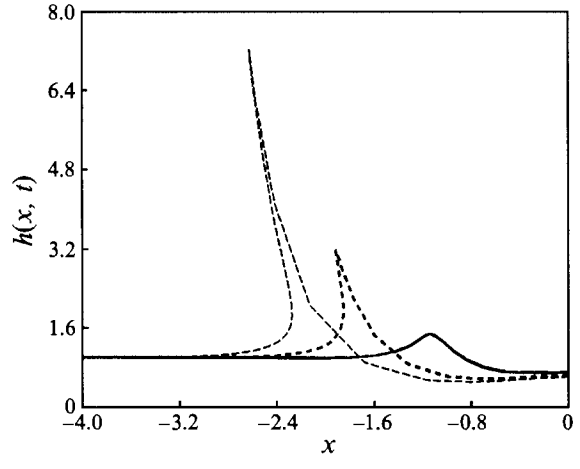

FIGURE 7. Case (i) breaking, $A = 1$, $P_1 = 4$, $S = 4$. Curves as for figure 6.

and eventually, owing to depletion of the alcohol source, flow stops. Figure 7, where $P_1 (= \chi H/\mu D_g)$ has been increased, shows that the outer side of the wave steepens and, in fact, eventually breaks. Thus increasing, for example, the Marangoni stresses χ eventually leads to breaking. In a sense P_1 acts as a bifurcation parameter, loosely speaking, in this instance defining whether or not the wave breaks. In §7, it was suggested that increasing P_1 should lead to wave breaking: in the present instance the critical value occurs at about $P_1 = 3$. This can be viewed in terms of the viscosity of the liquid: if the liquid is very viscous, breaking never occurs as the shear stresses are dissipated in the liquid; as μ decreases a critical point is reached whereupon the dissipation is too small to prevent the liquid piling up on itself and finally breaking. For $P_1 = 4$, the time to breaking is about 1.0. However, we can obtain a so-called shock solution of (57), (58) by using the rule of equal areas (Whitham 1974). This removes multivaluedness from solutions such as those in figure 7 by inserting a vertical wave (shock) profile in such a way as to make the cut-off areas equal ($\int h\,dx$ is conserved, see for example figure 12). Furthermore, as we shall see, these solutions are indeed very close to the 'exact' solutions to be attained in §§11.2.1 and 11.2.2 and may be considered 'outer' solutions.

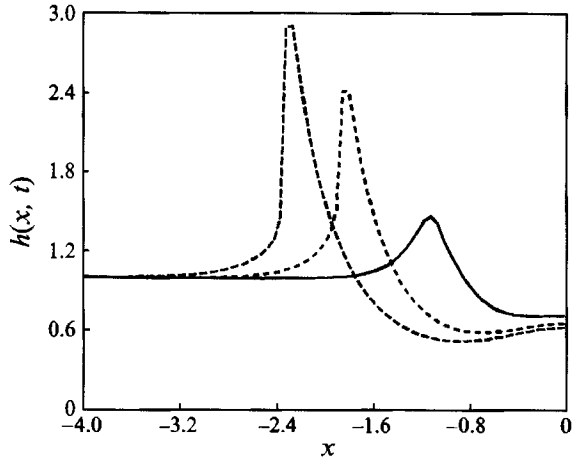

FIGURE 8. Case (ii) breaking, $A = 1$, $P_1 = 4$, $S = 4$, $\epsilon^2 B = 0.001$. Curves as for figure 6.

11.2. *Solutions with smoothing*

11.2.1. *Case (ii): Marangoni flow with gravity smoothing*

In this instance the $O(\epsilon^2 B)$ terms of (27) are included but ϵ remains zero. Although in real situations, surface tension almost always plays a dominant role, it is interesting to compare results obtained with and without its effects. We thus need to solve a second-order parabolic partial differential equation obtained by setting $\epsilon = 0$ in (27) which we rewrite here for convenience:

$$h_t = \tfrac{1}{2}\gamma_{xx} h^2 + \gamma_x h h_x + \epsilon^2 B(\tfrac{1}{3} h_{xx} h^3 + h^2 h_x^2). \tag{60}$$

To solve this equation, an initial condition and two boundary conditions are required, which can be expressed as

$$h(x, 0) = 1, \tag{61}$$

$$\partial h/\partial x = 0 \quad \text{at} \quad x = \pm\infty, \tag{62}$$

the last condition expressing the fact that the free surface remains horizontal at ∞. Replacing this condition by $h(\pm\infty, t) = 1$ gave essentially the same results. The numerical method of lines, whereby the x-derivatives are discretized resulting in a system of ordinary differential equations, was used. Different tolerances for the time differentiation were used up to 10^{-5} in some cases though there was generally no discernible difference between results for a tolerance of 10^{-3} and 10^{-5}. For the x-derivatives different step lengths were tested and the solutions appeared to converge well. In general a step size of 5×10^{-2} was adequate for the parameter ranges under consideration though in the neighbourhood of a shock a finer grid was necessary depending on the size of $\epsilon^2 B$. Referring to (60) we expect the formation of a shock to be prevented by the $\partial^2 h/\partial x^2$ terms. The results of §9 indicate that a step size of about $\epsilon^2 B$ is necessary to resolve such a shock. In order to save computational time, the position of the shock can be determined by a consideration of the 'outer' solutions of §11.1. In this way a finer grid can be positioned wherever shock formation is occurring.

We consider the same basic situations as before. Beginning with the no-breaking situation, the case corresponding to figure 6 with $\epsilon^2 B = 0.1$ gave results very similar to figure 6 with slightly flatter profiles. Figure 8 corresponds to the breaking case of figure 7 for very small $\epsilon^2 B$ and it is evident that the wave peak resembles the case (i) solutions

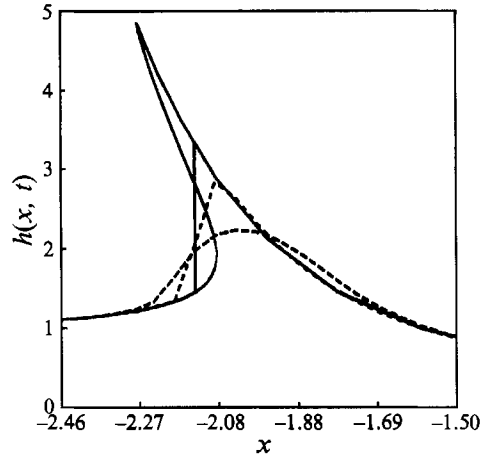

FIGURE 9. Comparison of case (i) and case (ii) for decreasing $\epsilon^2 B$. $A = 1$, $P_1 = 4$, $S = 4$. The case (i) situation has an 'equal areas' vertical line introduced to represent a shock solution. ——, Case (i), $\epsilon^2 B = 0$; – – –, case (ii), $\epsilon^2 B = 0.001$; — — —, case(ii), $\epsilon^2 B = 0.01$.

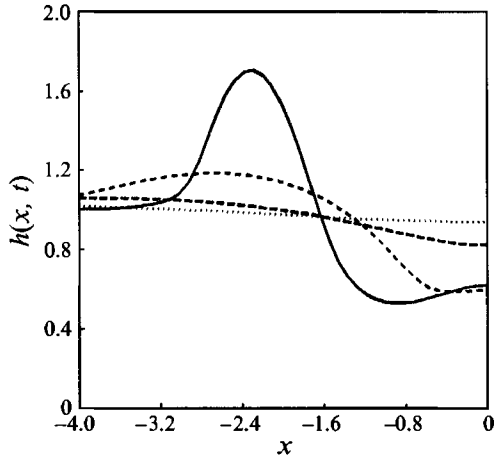

FIGURE 10. Recovery of free surface under action of gravity after source is removed. $A = 1, 0$, $P_1 = 4$, $S = 4$, $\epsilon^2 B = 0.1$. ——, $t = 2$, $(A = 1)$; – – –, $t = 10$ (no source); — — —, $t = 50$ (no source); ·····, $t = 120$ (no source).

but never breaks. In §9, the smoothing-layer thickness was predicted to be $O(\epsilon^2 B)$ which is 0.001 for the case illustrated in figure 8. The smoothing effect of the gravity terms is well illustrated in figure 9, where the effect of decreasing the value $\epsilon^2 B$ in case (ii) is compared to the corresponding case (i) solution where a shock has been inserted according to the equal areas rule. Note that as $\epsilon^2 B \to 0$ the smoothed case (ii) solution appears to approach the shock case (i) solution.

Figure 10 shows a situation where recovery of the free interface occurs. In this instance a source ($A = 1$) is present from $t = 0$ to $t = 2$. A typical wave forms and moves outwards. At $t = 2$, the source is removed ($A = 0$) and the liquid is allowed to fall back in on itself under the action of gravity alone (in this instance) where $\epsilon^2 B$ is quite large. Note that during recovery the liquid level at $x = 0$ first falls before rising as the trough located at about $x = -1$ is filled, initially from both sides. We comment

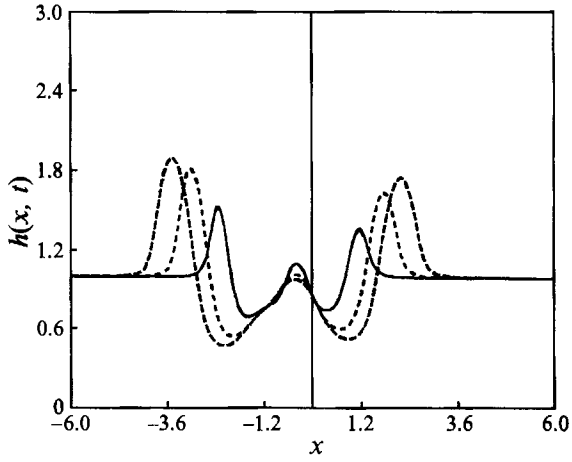

FIGURE 11. Free surface in the presence of two alcohol sources at $x = 0, -1$, $A = 1, 2$, $P_1 = 4$, $S = 4$, $\epsilon^2 B = 0.1$. ——, $t = 0.6$; – – –, $t = 1.2$; ———, $t = 1.8$.

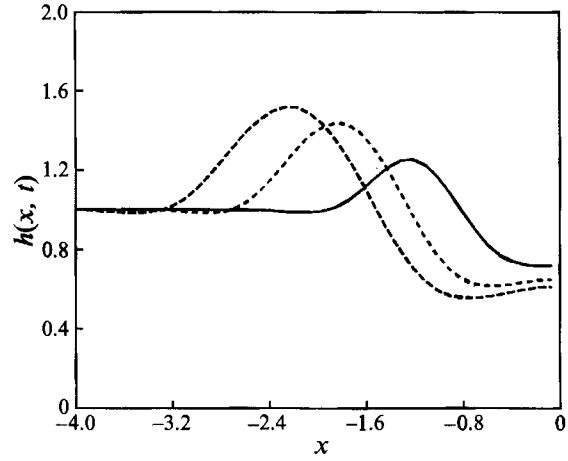

FIGURE 12. Case (iii) breaking, $A = 1$, $P_1 = 4$, $S = 4$, $\epsilon^2 B = 0.1$, $\epsilon = 0.1$. ——, $t = 0.6$; – – –, $t = 1.2$; ———, $t = 1.8$.

also that the equation governing the recovery problem requires rescaling ($p_r = p^*/\rho g H$, $u_r = u^* \mu L/\rho g H^3$ – illustrating very slow recovery for small H – and $t_r = \rho g H^3 t^*/\mu L^2$) resulting in a nonlinear diffusion equation: $h_t = \frac{1}{3}[h^3 h_x]_x$.

Figure 11 gives an illustration of the possibilities for creating different interface shapes. In this instance a second source of strength 2 has been placed at $x = -1$ and the wave profile calculated. The results are of course no longer symmetrical about $x = 0$.

11.2.2. *Case (iii): Marangoni flow, gravity, surface-tension smoothing*

In this instance, we include all the terms of (27). When compared with case (ii), the results are qualitatively similar. For the situation corresponding to figure 6 with no breaking, the plots (not reproduced here) are very similar. Proceeding to breaking situations, figure 12, for quite large surface tension ($\epsilon = 10^{-1}$), does not come close to breaking while small oscillations develop downstream. In figure 13 ϵ has been decreased giving rise to a higher thinner peak. Note that the oscillations have more or

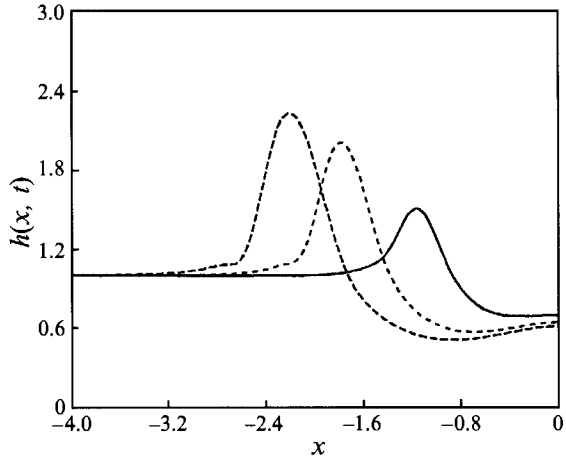

FIGURE 13. Case (iii) breaking, $A = 1$, $P_1 = 4$, $S = 4$, $\epsilon^2 B = 0.01$, $\epsilon = 0.01$. Curves as in figure 12.

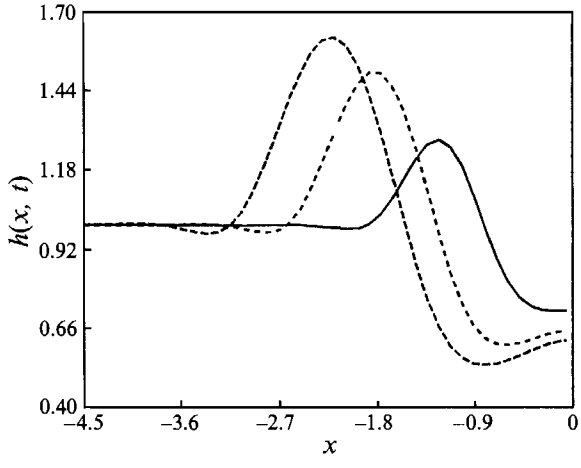

FIGURE 14. Evolution of the free surface with surface tension as the only smoothing process. $A = 1$, $P_1 = 4$, $S = 4$, $\epsilon^2 B = 0$, $\epsilon = 0.1$. Curves as in figure 12.

less disappeared suggesting that they are caused by the surface-tension terms. The analysis of §9 indicated that the smoothing-layer thickness is $O(\epsilon^{\frac{2}{3}}) \approx 0.21$ in figure 12, while its actual thickness looks to be about 0.6 (though figure 12 also suggests that more than simple smoothing-layer behaviour may occur here). In figure 13 the predicted smoothing-layer thickness is $(0.01)^{\frac{2}{3}} \approx 0.05$ while the actual thickness looks to be about 0.2.

Qualitatively the addition of surface-tension terms has modified the shock structure somewhat and produced slight changes in the global picture. In the analogous situation with the Korteweg–de Vries and Burgers equations, the different smoothing terms show quite different long-term behaviour in that the dispersive third-derivative terms of the former equation can lead to oscillations away from the steep region while the effect of the diffusive second-derivative terms of the latter remain localized at points where the profile steepens. For comparison we remove some of the second-derivative diffusive terms in (27) by setting $\epsilon^2 B = 0$. A typical result is shown in figure 14 where some slight oscillations can be seen downstream of the steepening wave. Similar oscillations were noted in figure 12 above. These are not numerical in origin; different

sized grids yield the same result. The situation bears some resemblance to that arising during the development of an undular bore (Peregrine 1966) or wave steepening in the Korteweg–de Vries equation with artificial (small) damping (Whitham 1974). In view of the analysis of §9 and in particular (36), we expect similar results for the case when $\epsilon = 0.1$, $B = 1$, because if §9 is correct, the $O(\epsilon^2 B)$ terms should remain negligible (i.e. $O(N)$ in the terminology of §5) in this case. Numerical solutions verify this, the results (not reproduced here) being virtually indistinguishable from figure 14 where $B = 0$.

Finally we comment that the case of recovery under the influence of gravity and surface tension (with $\epsilon^2 B = \epsilon = 0.1$) qualitatively resembles a flattened version of figure 10.

12. Concluding remarks

By the use of scaling arguments, we have reduced the problem of the evolution of a free liquid surface under the action of alcohol-vapour-induced Marangoni effects to a single nonlinear partial differential equation. The results only apply over a small portion of parameter space but this approach has allowed us to highlight the features of this type of flow for very thin films. A first-order partial differential equation models the process, at least qualitatively, even in the case where shocks arise and suitable discontinuities must be inserted. The concepts of boundary-layer ideas borrowed from singular perturbation theory are used to simplify the numerical problem. The resulting equation (27) can hardly be further simplified, yet is asymptotically correct to leading order.

An examination of the results indicates that solutions are divided into two main classes: breaking (in the theoretical sense) and non-breaking. The critical parameter controlling this process is $P_1 = \chi H / D_g \mu$. If this is large enough Marangoni stresses completely overcome viscous effects and smoothing effects become important.

Precise experimental verification of the model developed in this paper would not be easy. The emphasis here has been on asymptotic simplification while concentrating on just one small parameter: the aspect ratio, other parameters being assumed $O(1)$ unless otherwise noted. However, when the model was initially being developed, a number of bench-top experiments was carried out to help develop an understanding of the processes involved. The polished side of an approximately circular silicon wafer (radius 5 cm) was covered with a relatively thick water film for ease of observation. The average film thickness, estimated by weighing, was about 9 μm. A drop of isopropanol was then suspended from the end of a pipette at a distance of about 1 cm above the water surface. A more or less circular wave was seen to develop and more radially outwards centred about the point directly below the alcohol drop and leaving a thinner film behind. The characteristic speed of propagation was estimated to be about 1 cm s^{-1}. Though lacking refinement, this experiment does allow us to check if the scales in (10) are reasonable. Taking $\mu = 10^{-3}$ Kg m^{-1} s^{-1}, $L = 1$ cm, $\chi = 4 \times 10^{-2}$ Nm^{-1}, $H = 10$ μm, we obtain a characteristic timescale of about 0.25 s and characteristic velocity of about 4 cm s^{-1}, so the balances represented in (10) appear correct.

Further work in this area will include consideration of dip-coating-type problems in the presence of alcohol vapour as in figure 1. This problem is rather more difficult than that considered in this paper as the curvature of the liquid free surface will play an important role in the diffusion of the alcohol into the liquid. It is clear that gravity will play no role in the smoothing out of possible discontinuities: this can only be carried out by surface tension and may lead to qualitatively different shock structures than obtained in this paper.

The author acknowledges useful discussions with Dr A. B. Tayler and Dr A. C. Fowler.

REFERENCES

BENNEY, D. J. 1966 Long waves in liquid films. *J. Math. & Phys.* **45**, 150.

GAVER, D. P. & GROTBERG, J. B. 1990 The dynamics of a localized surfactant on a thin film. *J. Fluid Mech.* **213**, 127.

HALPERN, D. & GROTBERG, J. B. 1992 Dynamics and transport of a localized soluble surfactant on a thin film. *J. Fluid Mech.* **237**, 1.

HANSEN, R. S. 1960 The theory of diffusion controlled absorption kinetics with accompanying evaporation. *J. Colloid Si.* **64**, 637.

HAYDON, R. 1958 An investigation of droplet oscillation during mass transfer. *Proc. R. Soc. Lond.* A **243**, 483.

JENSEN, O. E. & GROTBERG, J. B. 1992 Insoluble surfactant spreading on a thin viscous film; shock evolution and film rupture. *J. Fluid Mech.* **240**, 259.

KEVORKIAN, J. & COLE, J. D. 1981 *Perturbation Methods in Applied Mathematics.* Springer.

LEENAARS, A. F. M., HUETHORST, J. A. M. & OEKEL, J. J. VAN 1991 Marangoni drying: a new extremely clean process. *Langmuir* **7**, 2748.

LEVICH, V. G. & KRYLOV, V. S. 1969 Surface tension driven phenomena. *Ann. Rev. Fluid Mech.* **1**, 293.

MARANGONI, C. G. M. 1871 *Ann. Phys. (Poggendorff)* **143**, 337.

MORIARTY, J. A., SCHWARTZ, L. W. & TUCK, E. O. 1991 Unsteady spreading of thin liquid films with small surface tension. *Phys. Fluids* A **3**, 733.

MYSHKIS, A. D. 1986 *Low Gravity Fluid Mechanics.* Springer.

OVERDIEP, W. S. 1986 The levelling of paints. *Prog. Organic Coatings* **14**, 159.

PATBERG, W. B., KOERS, A., STEENGE, W. D. E. & DRINKENBURG, A. A. H. 1983 *Chem. Engng Sci.* **38**, 917.

PEREGRINE, D. H. 1966 Calculations of the development of an undular bore. *J. Fluid Mech.* **25**, 321.

PIMPUTKAR, S. M. & OSTRACH, S. 1980 Transient thermocapillary flow in thin liquid layers. *Phys. Fluids* **23**, 1281.

SCRIVEN, L. E. & STERNLING, C. V. 1960 The Marangoni effects. *Nature* **187**, 186.

THOMSON, J. 1855 *Phil. Mag.* (4) **10**, 330.

WHITHAM, G. B. 1974 *Linear and Nonlinear Waves.* John Wiley & Sons.